

$K^+ \rightarrow \pi^+\pi^0\gamma$ in the Standard Model and Beyond

P. MERTENS

*Centre for Cosmology, Particle Physics and Phenomenology (CP3)
Université catholique de Louvain, Chemin du Cyclotron, 2
B-1348 Louvain-la-Neuve, Belgium*

In this note we show how improved theoretical analysis combined with recent experimental data coming from NA48/2 concerning $K^+ \rightarrow \pi^+\pi^0\gamma$ decay shed light on the dynamics of the $s \rightarrow d\gamma$ transition. Consequences on NP analysis are also presented.

1 Introduction

In the search for New Physics (NP) the $s \rightarrow d\gamma$ process is complementary to $b \rightarrow s\gamma$ and $\mu \rightarrow e\gamma$, as the relative strength of these transitions is a powerful tool to investigate the NP dynamics. However, since $s \rightarrow d\gamma$ takes place deep within the non-perturbative regime of QCD we have to control hadronic effects and find observables sensitive to the short-distance dynamics, and thereby to possible NP contributions. The purpose of this note is to show how this can be achieved using the $K^+ \rightarrow \pi^+\pi^0\gamma$ observable [1].

In section 2, the anatomy of the $s \rightarrow d\gamma$ process in the Standard Model (SM) is shortly detailed. In section 3, we analyse the $K^+ \rightarrow \pi^+\pi^0\gamma$ decay in the SM whereas section 4 is devoted to show how, in the MSSM, rare and $K^+ \rightarrow \pi^+\pi^0\gamma$ decays, as well as $\text{Re}(\varepsilon'_K/\varepsilon_K)$ can be exploited to constrain NP.

2 The $s \rightarrow d\gamma$ anatomy

In the SM, the flavour changing electromagnetic process $s \rightarrow d\gamma$ is a loop effects which at low energy scale is described by the effective $\Delta S = 1$ Hamiltonian [2]

$$\mathcal{H}_{eff}(\mu \approx 1 \text{ GeV}) = \sum_{i=1}^{10} C_i(\mu) Q_i(\mu) + C_{\gamma^*}^{\pm} Q_{\gamma^*}^{\pm} + C_{\gamma}^{\pm} Q_{\gamma}^{\pm} + h.c. , \quad (1)$$

where the Q_i are effective four-quarks operators whereas the quark-bilinear electric $Q_{\gamma^*}^{\pm}$ and magnetic Q_{γ}^{\pm} operators are respectively given by^a $Q_{\gamma^*}^{\pm} = (\bar{s}_L\gamma^{\nu}d_L \pm \bar{s}_R\gamma^{\nu}d_R) \partial^{\mu}F_{\mu\nu}$ and $Q_{\gamma}^{\pm} = (\bar{s}_L\sigma^{\mu\nu}d_R \pm \bar{s}_R\sigma^{\mu\nu}d_L) F_{\mu\nu}$. In the non perturbative regime of QCD this Hamiltonian is hadronized into an effective weak Lagrangian that shares the chiral properties of the operators contained in \mathcal{H}_{eff} . The chiral structures of Q_i and $Q_{\gamma^*}^{\pm}$ allow the usual $\mathcal{O}(p^2)$ weak Lagrangian $\mathcal{L}_W = G_8 O_8 + G_{27} O_{27} + G_{ew} O_{ew}$ (detailed in [10]) whereas the chirality flipping Q_{γ}^{\pm} operators induce more involved $\mathcal{O}(p^4)$ local interactions (detailed in [1,10]). The non-trivial dynamics corresponding to

^aBy definition : $2\sigma^{\mu\nu} = i[\gamma^{\mu}, \gamma^{\nu}]$.

the low-energy tails of the photon penguins arise at $\mathcal{O}(p^4)$ (the $\mathcal{O}(p^2)$ dynamics being completely predicted by Low's theorem [3]) where they are represented in terms of non-local meson loops, as well as additional $\mathcal{O}(p^4)$ local effective interactions, in particular the $\Delta I = 1/2$ enhanced N_{14}, \dots, N_{18} octet counterterms [4, 5].

3 $K^+ \rightarrow \pi^+\pi^0\gamma$ in the SM

For the $K^+ \rightarrow \pi^+\pi^0\gamma$ decay, the standard phase-space variables are chosen as the π^+ kinetic energy T_c^* and $W^2 \equiv (q_\gamma \cdot P_K)(q_\gamma \cdot P_{\pi^+})/m_{\pi^+}^2 m_K^2$ [6]. Indeed, pulling out the dominant bremsstrahlung contribution, the differential rate can be written

$$\frac{\partial^2 \Gamma}{\partial T_c^* \partial W^2} = \frac{\partial^2 \Gamma_{IB}}{\partial T_c^* \partial W^2} \left(1 - 2 \frac{m_{\pi^+}^2}{m_K} \operatorname{Re} \left(\frac{E_{DE}}{eA_{IB}} \right) W^2 + \frac{m_{\pi^+}^4}{m_K^2} \left(\left| \frac{E_{DE}}{eA_{IB}} \right|^2 + \left| \frac{M_{DE}}{eA_{IB}} \right|^2 \right) W^4 \right). \quad (2)$$

In this expression both electric E_{DE} and magnetic M_{DE} direct emission amplitudes are functions of W^2 and T_c^* and appear at $\mathcal{O}(p^4)$. To a very good approximation we can identify these direct emission amplitudes with their first multipole for which the $\pi^+\pi^0$ state is in a P wave. The main interest of $K^+ \rightarrow \pi^+\pi^0\gamma$ is that its bremsstrahlung component $A_{IB} = A(K^+ \rightarrow \pi^+\pi^0)$ is pure $\Delta I = 3/2$ hence suppressed, making the direct emission amplitudes easier to access. The magnetic amplitude M_{DE} is dominated by the QED anomaly and will not concern us here.

3.1 Differential rate

Given its smallness, we can assume the absence of CP-violation when discussing this observable. Experimentally, the electric and magnetic amplitudes (taken as constant) have been fitted in the range $T_c^* \leq 80$ MeV and $0.2 < W < 0.9$ by NA48/2 [7]. For the electric amplitude, using their parametrization, we obtain at $\mathcal{O}(p^4)$:

$$X_E = \frac{-\operatorname{Re}(E_{DE}/eA_{IB})}{m_K^3 \cos(\delta_1^1 - \delta_0^2)} = \frac{3G_8/G_{27}}{40\pi^2 F_\pi^2 m_K^2} \left[E^l(W^2, T_c^*) - \frac{m_K^2 \operatorname{Re} \bar{N}}{m_K^2 - m_\pi^2} \right] \equiv X_E^l - X_E^{CT}, \quad (3)$$

where δ_1^1 (δ_0^2) is the strong phase of E_{DE} (A_{IB}). The E^l represents O_8 and O_{27} induced loop contributions (loop contributions from O_{ew} are sub-leading) and \bar{N} corresponds to local counterterms and Q_γ^- contributions. Naively we would expect the O_{27} contributions to be sub-dominant, however, they are dynamically enhanced by $\pi\pi$ loops. Since experimentally, no slope were included in X_E , we average E^l over the experimental range and find $X_E^l = -17.6 \text{ GeV}^{-4}$. Knowing X_E^l and using the experimental measurement of $X_E = (-24 \pm 4 \pm 4) \text{ GeV}^{-4}$ we can extract the local contributions

$$X_E^{CT}/X_E^l = 0.37 \pm 0.32 \quad \rightarrow \quad \operatorname{Re} \bar{N} = 0.095 \pm 0.083. \quad (4)$$

To our knowledge it is the first time that $K^+ \rightarrow \pi^+\pi^0\gamma$ counterterms contributions are extracted from experiment. The value we found is much smaller than the $\mathcal{O}(1)$ expected for the N_i on dimensional grounds or from factorization [8]. Note that the required amount of counterterm contribution would have been bigger if O_{27} loops were neglected since then $X_E^l = -10.2 \text{ GeV}^{-4}$. This result is important since it implies that the counterterms combination \bar{N} , which appears in other radiative K decays, is now under control and further reliable theoretical investigations can be carried on, in particular concerning the CP violating observables.

3.2 Direct CP-violating asymmetry

Since the bremsstrahlung and direct emission amplitudes interfere and carry different strong and weak phases, a non vanishing CP violating asymmetry can be generated. The asymmetry measures direct CP violation since K^\pm do not mix. Besides and because the long-distance bremsstrahlung amplitude dominates the branching, this CP asymmetry is the simplest window on short-distance physics and a fortiori on possible NP effects. CP-violation in $K^+ \rightarrow \pi^+\pi^0\gamma$ is quantified by the parameter $\varepsilon'_{+0\gamma}$, defined from

$$\text{Re}\left(\frac{E_{DE}}{eA_{IB}}\right)(K^\pm \rightarrow \pi^\pm\pi^0\gamma) \approx \frac{\text{Re } E_{DE}}{e \text{Re } A_{IB}} [\cos(\delta_1^1 - \delta_0^2) \mp \sin(\delta_1^1 - \delta_0^2)\varepsilon'_{+0\gamma}] , \quad (5)$$

as $\varepsilon'_{+0\gamma} \equiv \text{Arg}E_{DE} - \text{Arg}A_{IB}$ (see [9]). Both Q_γ^- and Q_i (through loops and counterterms) contribute to this parameter and we find

$$\varepsilon'_{+0\gamma}(Q_i) = -0.55(25)\frac{\sqrt{2}|\varepsilon'_K|}{\omega} \quad \text{and} \quad \varepsilon'_{+0\gamma}(Q_\gamma^-) = +2.8(7)\frac{\text{Im } C_\gamma^-}{G_F m_K} , \quad (6)$$

respectively^b. Sadly, these contributions interfere destructively implying that $\varepsilon'_{+0\gamma}|_{\text{SM}} = 0.5(5) \times 10^{-4}$. This large uncertainty is driven by a large uncertainty on counterterms and on estimated $\mathcal{O}(p^6)$ effects. However, contrary to what happens in ε'_K , $\varepsilon'_{+0\gamma}$ is rather insensitive to isospin breaking effects, conservatively taken into account in (6). Expressing $\varepsilon'_{+0\gamma}(Q_i)$ in term of the experimental ε'_K allows us to keep possible NP effects in Q_i under control. As a consequence, the only way for NP to affect $\varepsilon'_{+0\gamma}$ is via its $\text{Im } C_\gamma^-$ component. The current bound obtained by NA48/2 [7] is rather weak and allows very large NP effects in $\varepsilon'_{+0\gamma}$:

$$\text{Im } C_\gamma^-|_{NP}/G_F m_K = -0.08 \pm 0.13 . \quad (7)$$

4 $K^+ \rightarrow \pi^+\pi^0\gamma$ beyond the SM

Once combined with other short-distance sensitive observables, any experimental improved measurement of $\varepsilon'_{+0\gamma}$ will be greatly rewarding. The main problem when probing NP is the issue of disentangling correlations between various NP sources in a fully model-independent way. In [10], we analysed broad classes of NP scenarios defined as model-independently as possible and identified corresponding strategies to constrain and disentangle NP sources using experimental informations on $K_L \rightarrow \pi\ell^+\ell^-$, $K \rightarrow \pi\nu\bar{\nu}$ decays and $\text{Re}(\varepsilon'_K/\varepsilon_K)$. Doing so we highlighted the complementary informations that could be obtained from radiative decays.

In the MSSM [11–16], NP can affect all the operators in (1) as well as gluon-penguin (denoted by Q_g^\pm) and semi-leptonic operators, in particular $Q_{V,l} = \bar{s}\gamma_\mu d \otimes \bar{\ell}\gamma^\mu \ell$. In this particular model the irreducible correlations are two fold. First Q_γ^+ and $Q_{V,l}$ ($\ni Q_{\gamma^*}^+$) always interfere in $K_L \rightarrow \pi\ell^+\ell^-$ in and beyond the SM and second, $\text{Re}(\varepsilon'_K/\varepsilon_K)$ receives NP contributions from many different sources. The corresponding bounds are displayed in Figure 1 where we see that a large but not impossible cancellation between NP in gluon-penguin and electroweak operators in $\text{Re}(\varepsilon'_K/\varepsilon_K)$ allows for $\text{Im}C_\gamma^+$ to reach the percent level if we impose $\text{Im}C_\gamma^+ = \pm 1.5 \text{Im}C_g^-$. This value will correspond to a saturation of the current $K_L \rightarrow \pi^0 e^+ e^-$ upper bound and since in the MSSM Q_γ^\pm and Q_g^\pm mix under renormalization this $\text{Im}C_\gamma^+$ upper bound provides also an lower bound for $\text{Im}C_\gamma^-$. From (6) this implies that NP can push $\varepsilon'_{+0\gamma}$ up to roughly two orders of magnitude above its SM prediction. The parameter $\varepsilon'_{+0\gamma}$ provides therefore a very good probe for NP γ -penguin effects and furthermore reveals NP cancellations occurring inside $\text{Re}(\varepsilon'_K/\varepsilon_K)$.

^b Numerically, in the SM, the Wilson coefficient of the magnetic operator in $b \rightarrow s\gamma$ can be used for $\text{Im}C_\gamma^\pm$, since the CKM elements for the u , c , and t contributions scale similarly and we find $\text{Im}C_\gamma^\pm(2 \text{ GeV})_{\text{SM}}/G_F m_K = \mp 0.31(8) \times \text{Im} \lambda_t$.

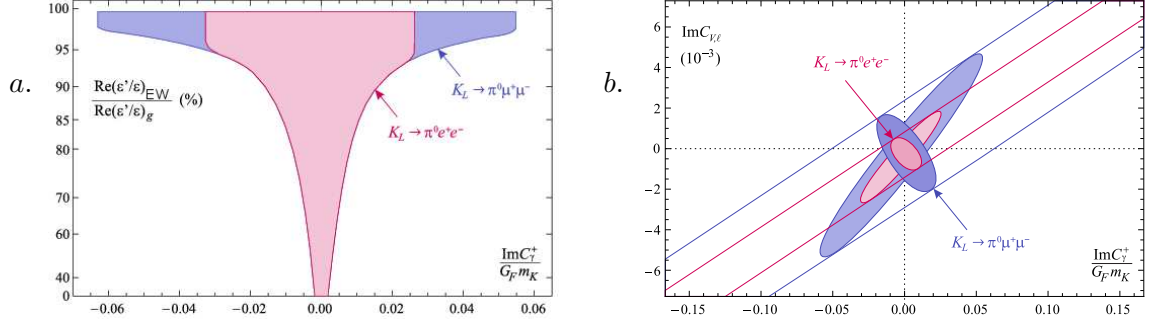


Figure 1: Loop-level FCNC scenario, with all the electroweak operators as well as $Q_{\gamma,g}^\pm$ simultaneously turned on, but imposing $\text{Im}C_\gamma^+ = \pm 1.5 \text{Im}C_g^-$ and $|\text{Re}(\epsilon'_K/\epsilon_K)^{\text{NP}}| < 2 \text{Re}(\epsilon'_K/\epsilon_K)^{\text{exp}}$. (a) The $\text{Im}C_\gamma^+$ range as a function of the fine-tuning between $\text{Re}(\epsilon'_K/\epsilon_K)_{EW}$ and $\text{Re}(\epsilon'/\epsilon)_g$. (c) The corresponding contours in the $\text{Im}C_{V,\ell} - \text{Im}C_\gamma^+$ plane. In (b), the lighter (darker) colors denote destructive (constructive) interference between NP γ^* -penguin and Q_γ^+ in $K_L \rightarrow \pi^0 \ell^+ \ell^-$.

5 Conclusion

We exemplify in $K^+ \rightarrow \pi^+ \pi^0 \gamma$ that the stage is now set theoretically to fully exploit the $s \rightarrow d \gamma$ transition. The SM predictions are under good control, the sensitivity to NP is excellent, and signals in rare and radiative K decays not far from the current experimental sensitivity are possible. Thus, with the advent of the next generation of K physics experiments (NA62 at CERN, KOTO at J-Parc, ORKA at Fermilab and KLOE-II at the LNF), the complete set of flavor changing electromagnetic processes, $s \rightarrow d \gamma$, $b \rightarrow (s, d) \gamma$, and $\ell \rightarrow \ell' \gamma$, could become one of our main windows into the flavor sector of the NP which will hopefully show up at the LHC.

Acknowledgments

I thank the organizers of the *Rencontres de Moriond EW 2012* for the pleasant and stimulating stay and for their financial support. I warmly thank Christopher Smith for the fruitful collaboration at the origin of this work. I'm also grateful to him and Jean-Marc Gérard for their valuable suggestions and comments about the present note.

References

1. G. Colangelo, G. Isidori and J. Portoles, Phys. Lett. B **470** (1999) 134.
2. G. Buchalla, A. J. Buras and M. E. Lautenbacher, Rev. Mod. Phys. **68** (1996) 1125.
3. F. E. Low, Phys. Rev. **110** (1958) 974.
4. J. Kambor, J. H. Missimer and D. Wyler, Nucl. Phys. B **346** (1990) 17.
5. G. Ecker, J. Kambor and D. Wyler, Nucl. Phys. B **394** (1993) 101.
6. N. Christ, Phys. Rev. **159** (1967) 1292.
7. J. R. Batley *et al.* [NA48/2 Collaboration], Eur. Phys. J. C **68** (2010) 75.
8. G. Ecker, H. Neufeld and A. Pich, Nucl. Phys. B **413** (1994) 321.
9. G. D'Ambrosio and G. Isidori, Int. J. Mod. Phys. A **13** (1998) 1.
10. P. Mertens and C. Smith, JHEP **1108** (2011) 069.
11. A. J. Buras and L. Silvestrini, Nucl. Phys. B **546** (1999) 299.
12. A. J. Buras *et al.*, Nucl. Phys. B **566** (2000) 3.
13. F. Mescia, C. Smith and S. Trine, JHEP **0608** (2006) 088.
14. G. Colangelo and G. Isidori, JHEP **9809** (1998) 009.
15. G. Isidori, F. Mescia, P. Paradisi, C. Smith and S. Trine, JHEP **0608** (2006) 064.
16. A. J. Buras, T. Ewerth, S. Jager and J. Rosiek, Nucl. Phys. B **714** (2005) 103.